

# Effect of aqueous solvation on the structures of pyruvic acid isomers and their reactions in solution: a computational study

Rita Kakkar<sup>a\*</sup>, Mallika Pathak<sup>a</sup> and Pragya Gahlot<sup>a</sup>



The pyruvic acid molecule and its various isomers have been studied in aqueous solution in order to understand the mechanism of decarboxylation. The tautomeric equilibrium remains in favor of the keto form in aqueous solution, but the energy difference between the two tautomers decreases. The anion also exists in the keto form in aqueous solution. Good agreement between the calculated and observed gas phase protonation and basicity values is obtained, and the calculated  $pK_a$  value is also in reasonable agreement with the literature value. The importance of the catalytic mechanism may be gauged from the fact that, in the absence of an enzymatic pathway, the reaction has high activation barrier and may not occur at all. Copyright © 2007 John Wiley & Sons, Ltd.

Supplementary electronic material for this paper is available in Wiley InterScience at <http://www.mrw.interscience.wiley.com/suppmat/0894-3230/suppmat/>

**Keywords:** pyruvic acid; decarboxylation; DFT; aqueous solvation; tautomerism

## INTRODUCTION

Pyruvic acid is one of the most important molecules biochemically, as it plays a fundamental role in biological systems, and occurs naturally in the body. It is an intermediate in the metabolism of carbohydrates, formed by the anaerobic glycolysis of glucose. It is then oxidized to carbon dioxide and acetate bonded to the coenzyme A (CoA). Its anion, pyruvate ( $\text{CH}_3\text{COCOO}^-$ ), is also an important intermediate compound in the carbohydrate metabolism of living organisms, and is the product of glycolysis and a precursor for the Krebs cycle.

Several authors have investigated the gas phase chemistry of pyruvic acid.<sup>[1–6]</sup> Our previous calculations at the Density Functional Theory (DFT) level<sup>[1]</sup> were also confined to the gas phase pyruvic acid molecule. We had investigated in detail the ground state conformation of the molecule and its reactions in the gas phase. It was found that a keto form with *trans*  $\text{C}_{\text{methyl}}\text{C}_{\text{keto}}\text{C}_{\text{acid}}\text{O}_{\text{hydroxyl}}$  and *cis*  $\text{C}_{\text{keto}}\text{C}_{\text{acid}}\text{OH}$ , and with one methyl hydrogen in a synperiplanar position with respect to the keto oxygen, is the most stable. This agrees with previous theoretical and experimental findings. Decarboxylation via three different possible routes was also studied. At the B3LYP/6-311++G(3df, 3pd) level, it was found that the direct formation of acetaldehyde, the most stable of the resulting  $\text{C}_2\text{H}_4\text{O}$  isomers, via a four-center-like transition state is the most feasible reaction, although there is a high activation barrier of 70 kcal/mol. This is in contrast to semiempirical calculations, which had found that a hydroxyethylidene–carbon dioxide complex is the most likely product as it is formed with very low activation energy. At the B3LYP/6-311++G(3df, 3pd) level, it was found that no hydroxyethylidene–carbon dioxide complex exists as a product, and no transition state leading to the dissociation to hydroxyethylidene could be located.

However, the bulk of the reactions of pyruvic acid occur in an aqueous milieu and it is interesting to investigate whether any

changes in the reaction scheme occur when solvation is taken into account. Moreover, direct extrapolation of gas phase results to realistic chemical systems cannot be made because of the different relative permittivities *in vacuo*, in biomolecules, and in water solutions. In the present work, the DFT method is used for the calculations performed on the pyruvic acid system for aqueous solutions.

Since this paper specifically concerns the aqueous chemistry of pyruvic acid, we have considered the treatment of solvent water molecules in some detail. Normally, for DFT calculations, the continuum approach is used to model the solvent. However, some recent studies have shown that such a treatment is not adequate. In the case of amino acids and peptides, it was found that some structures that do not exist in the gas phase become stable in solution due to their ability to form strong intermolecular hydrogen bonds with water.<sup>[7]</sup> Due to the phenomenal cost of treating all water molecules of even just the first solvation shell explicitly in a DFT calculation, we turned to semiempirical methods for treatment of the solvent in the case of thiohydroxamic acids. This resulted in final structures that have only a few water molecules directly bonded to the substrate molecule with hydrogen bonds. A DFT calculation with only these water molecules treated explicitly and the rest of the solvent treated as a continuous dielectric resulted in better agreement with experiment.<sup>[8]</sup> This approach has the added advantage that distortions in geometries of the substrate molecule to accommodate the hydrogen-bonded water molecules are adequately taken care of. In this paper, we have used this approach for

\* Department of Chemistry, University of Delhi, Delhi-110 007, India.  
E-mails: rkakkar@chemistry.du.ac.in; rita\_kakkar@vsnl.com

a R. Kakkar, M. Pathak, P. Gahlot  
Department of Chemistry, University of Delhi, Delhi-110 007, India

modeling the reactions and energies of tautomers of the pyruvic acid molecule.

## COMPUTATIONAL METHODS

The same methodology was adopted in the calculations reported here as for the gas phase calculations.<sup>[1]</sup> The DFT calculations were performed using the B3LYP three-parameter density functional, which includes Becke's gradient exchange correction,<sup>[9]</sup> the Lee, Yang, Parr correlation functional,<sup>[10]</sup> and the Vosko, Wilk, Nusair correlation functional.<sup>[11]</sup>

The geometries were fully optimized with respect to the energy using the basis set 6-31+G(d, p) and single-point calculations were performed with the 6-311++G(3df, 3pd) basis set using the Gaussian 03W suite<sup>[12]</sup> of programs. Initial geometries were taken from the gas phase optimized structures.

The influence of solvent on the relative stability of conformers was studied at two levels: firstly with discrete water molecules, and secondly by examining the effect of bulk solvent on the hydrated structures using a continuum model. For the first type of calculations, the starting positions of water molecules were carefully selected. Using the Hyperchem 6.0 software suite,<sup>[13]</sup> first the desired conformer was placed in a periodic cubic box of side 10 Å, containing ~34 TIP3P<sup>[14]</sup> water molecules. After a geometry optimization using the PM3 Hamiltonian,<sup>[15]</sup> the box was equilibrated. A 100 ps Molecular Dynamics (MD) simulation, at 300 K using PM3 forces, was performed initially to equilibrate the system. A further 100 ps simulation was then performed. To ensure that most thermally accessible structures were sampled, the simulation was stopped every 10 ps and the configuration optimized. The least energy structure from amongst these was then selected for further calculations. No geometrical constraints were applied in the MD simulations. It was found that in both the *cis* conformers, rotation about the central C—C bond occurs yielding the *trans* conformers. Thus, only two conformers *Tce* and *Tte* remain in solution. After a geometry optimization, all water molecules within a proximity of 5 Å of the substrate molecule were retained, and a geometry optimization again performed. In both cases, it was found that only 14 water molecules remained in this region.

After obtaining these initial structures, further geometry optimizations were performed with the PM3 method. In all cases, it was found that only three of the water molecules remained closely bonded to the conformer in the final structure, forming intermolecular hydrogen bonds. Taking these structures with three hydrogen-bonded waters, further optimization at the B3LYP/6-31G(d) level resulted in one of the water molecules moving away from the vicinity of the substrate, yielding dihydrates. Vibrational analysis was performed to confirm the nature of the stationary points. The harmonic vibrational frequencies were scaled down by a factor of 0.9614<sup>[16]</sup> to account for anharmonicity and other factors. None of the structures was found to possess imaginary vibrational frequencies. The final energies of these dihydrates were calculated at the B3LYP/6-311++G(3df, 3pd)/B3LYP/6-31G(d) level. Zero-point energies, calculated at the B3LYP/6-31G(d) level and scaled by a factor of 0.9806,<sup>[16]</sup> were added to the energies calculated with the higher basis set.

The influence of bulk solvent on these water complexes was studied by the CPCM polarizable conductor calculation model implemented in Gaussian 03W<sup>[17,18]</sup> (keyword SCRF = CPCM),

with the dielectric constant ( $\epsilon$ ) taken as 78.39 for water at 298.15 K. In this approach, the solvation Gibbs free energy is given by the sum of the non-electrostatic contribution due to the creation of the solute cavity in the solvent and the electrostatic interaction between solute and solvent. In the CPCM model, the solvent is represented by a constant dielectric medium surrounding a cavity built around the solute. The cavity was built using the simple United Atom Topological (UA0) model applied on atomic radii of the universal force field (UFF). In this model, the radii of CH<sub>3</sub>, C, O, and OH are taken as 2.525 Å, 1.925 Å, 1.750 Å, and 1.850 Å, respectively. The calculations were performed with tesserae of 0.2 Å<sup>2</sup> average size.

## RESULTS AND DISCUSSION

Optimized Cartesian coordinates, energy values, and vibrational frequencies are given as Electronic Supplementary Information.

### Intermolecular hydrogen bonding

The same nomenclature and atom numbering (Fig. 1) is used for the pyruvic acid isomers as for the gas phase calculations.<sup>[1]</sup>

We first considered the role of two water molecules in stabilizing the various conformers of the keto form of pyruvic acid by hydrogen bonding. Details of obtaining the initial structures are given in the computational details section. The structures of the dihydrates are depicted in Fig. 2. It may be argued that each structure represents one of the several possible hydrogen-bonded structures with water. However, we believe that the final geometry optimization at the B3LYP level with two explicit water molecules results in the global minimum. It is also apparent from Fig. 2 that, for *Tce* for example, this is perhaps the best hydrogen-bonded structure possible with two water molecules. Moreover, other starting structures either optimized to these structures or gave higher energy structures. For example, initial

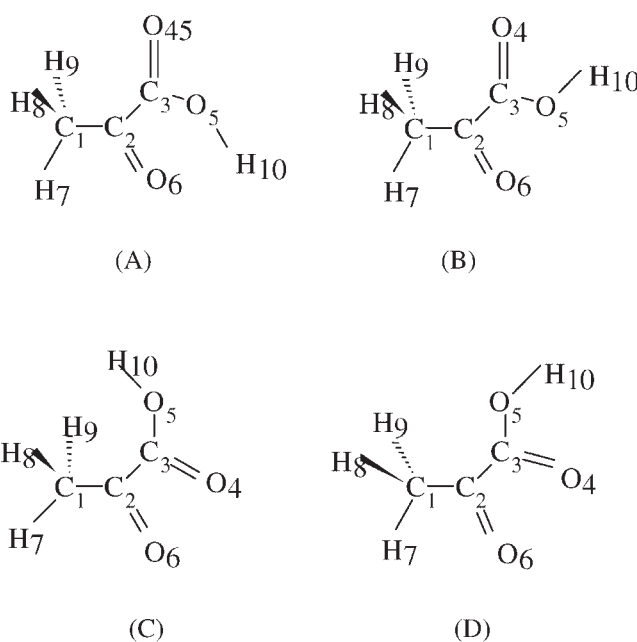


Figure 1. Conformers of pyruvic acid and atom numbering scheme (A): *Tce*; (B): *Tte*; (C): *Cce*; (D): *Cte*

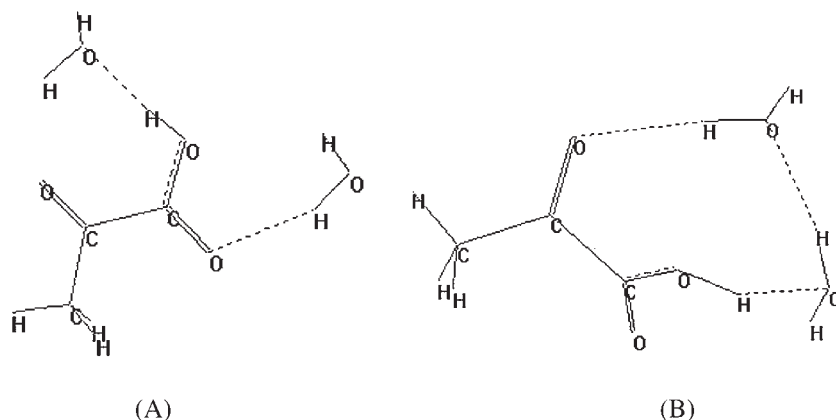


Figure 2. Structures of the two dihydrates (A): *Tce*; (B): *Tte*

placement of a water molecule hydrogen bonded to the —OH and C=O of the carboxylate group resulted in the water molecule moving toward the other water molecule, forming a stronger hydrogen bond with it. Experimentally, it is known that the ketone group hydrate of pyruvic acid is formed to an appreciable extent in aqueous solution by a rapidly established equilibrium reaction.<sup>[19]</sup>

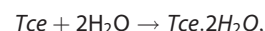
Despite the intramolecular hydrogen bonding in *Tce*, it is found that it forms a hydrogen-bonded hydrate with two water molecules, in which the carbonyl oxygen forms a close contact with a water hydrogen (1.98 Å), while the water oxygen is involved in hydrogen bonding with the carboxyl proton (1.67 Å). Both distances are much smaller than the sum of van der Waals radii of oxygen and hydrogen (2.72 Å). The respective O...H—O bond angles are found to be 134.8° and 174.2°, showing that the carboxyl proton forms strong linear hydrogen bonds (calculated bond order = 0.113) with water molecules. This weakens the carboxyl O—H bond, the calculated bond order being only 0.595. Moreover, the calculated NBO charges<sup>[20]</sup> on the hydroxyl oxygen and hydrogen are —0.702 and 0.522, respectively. The high values of the negative and positive charges also confirm the existence of hydrogen bonding.

The other hydrogen-bonded structure is *Tte*. $2\text{H}_2\text{O}$ . In this case, one water molecule forms a hydrogen bond with the carboxyl O—H, while the other forms a hydrogen bond with the carbonyl group, and the two are mutually hydrogen bonded. To accommodate the two water molecules, the two carbonyls have to twist out of plane, the dihedral angle being 115.4°. The carboxyl proton is hydrogen bonded to the water oxygen, the distance being 1.65 Å, while the distance of the carbonyl oxygen from a water hydrogen is 2.02 Å. Again, as for *Tce*, the carboxyl proton forms a stronger hydrogen bond than the oxygen. However, in this case, the bond is non-linear (151.1°). The hydrogen bond with the carbonyl oxygen spans 173.5°.

All the vibrational frequencies are found to be real, and this confirms that these are minima on the potential energy surface. The gas phase *Tce*. $2\text{H}_2\text{O}$  (energy after zero-point vibrational correction —495.353 893 6 Hartree) is found to be less stable than *Tte*. $2\text{H}_2\text{O}$  by 1.1 kcal/mol. In view of the fact that this difference is less than the B3LYP mean absolute deviation (MAD) for thermochemistry,<sup>[21]</sup> it cannot be said with certainty which of the two isomers predominates in solution. However, it may be stated that inclusion of two water molecules reduces the energy gap from 4.2 kcal/mol in the gas phase<sup>[1]</sup> to —1.1 kcal/mol. A possible

reason for this is the fact that stabilization due to the intramolecular hydrogen bonding present in the gas phase is lost due to the formation of intermolecular hydrogen bonds with water molecules in solution.

The calculated enthalpies for *Tce*, *Tte*,  $\text{H}_2\text{O}$ , *Tce*. $2\text{H}_2\text{O}$ , and *Tte*. $2\text{H}_2\text{O}$  at 298.15 K and 1 atm are, respectively, —342.460 570, —342.453 775, —76.439 432, —495.351 303, and —495.353 112 Hartree. These values were estimated by adding the thermal corrections to the energy to account for translational, vibrational, and rotational motion at 298.15 K and 1 atm. Thus, the reaction enthalpies for the processes



and



are calculated as —7.4 and —12.8 kcal/mol, respectively. Hence, hydrogen bonding with water stabilizes *Tte* to a greater extent than it does *Tce*. The corresponding free energy changes are, however, positive and the difference is smaller (8.8 and 7.8 kcal/mol, respectively). Thus, the entropic contributions, —54.3 and —69.1 cal K<sup>—1</sup> mol<sup>—1</sup>, respectively, are more unfavorable for the formation of the dihydrate of *Tte* (Fig. 2).

### Aqueous phase calculations

#### Keto forms

Before examining the effect of bulk solvent on these hydrated structures, let us examine what a simple continuum calculation on the isolated structures predicts. The effect of bulk water was considered by calculating the free energies of the various conformers in aqueous solution (see Table 1). For *Cce*, the optimization failed to converge unless the structure was constrained to a planar geometry. However, the planar conformation was found to possess an imaginary vibrational frequency (83 cm<sup>—1</sup>).

To validate the calculation procedure for the aqueous phase calculations, the results were computed at different levels of calculation. Table 1 reveals that, except *Cce*, for which the B3LYP/6-31G(d)//B3LYP/6-31G(d) calculation imposes an error of 1 kcal/mol, the relative free energies agree within  $\pm 0.1$  kcal/mol of each other. It may be noted that *Cce* is not an energy minimum in the sense that it possesses a small imaginary frequency, since the geometry had to be constrained to a planar conformation

**Table 1.** Calculated relative free energies (kcal/mol) of the various forms of pyruvic acid in aqueous solution

System	Relative free energy		
	6-31G(d)//6-31G(d)	6-311++G(3df, 3pd)//6-31G(d)	6-311++G(3df, 3pd)//6-311++G(3df, 3pd)
Tce	0.0 <sup>a</sup>	0.0 <sup>b</sup>	0.0 <sup>c</sup>
Tte	-0.7	-0.6	-0.5
Cce	7.8	6.8	6.9
Cte	-0.3	-0.4	-0.3

<sup>a</sup>  $G_{\text{soln}} = -342.402\ 053$  Hartree.  
<sup>b</sup>  $G_{\text{soln}} = -342.543\ 516$  Hartree.  
<sup>c</sup>  $G_{\text{soln}} = -342.544\ 148$  Hartree.

for the optimization to converge. We settled for the B3LYP/6-311++G(3df, 3pd)//B3LYP/6-31G(d) option for further calculations, as this gives a maximum error of only  $\pm 0.1$  kcal/mol compared to calculations with geometry optimization with the higher basis set at one-tenths of the computational cost.

We note that the implicit solvent model predicts that Cte is almost as stable as Tte (Table 1), whereas the explicit solvent calculation reveals that it undergoes rotation to the more stable Tte form. We therefore confined further aqueous phase calculations to the dihydrates of the two conformers Tce and Tte in a continuum of dielectric 78.39. This yielded the result that the dihydrate of Tte is slightly more stable than that of Tce (0.9 kcal/mol), but this small difference in energies is insignificant when compared with the MAD values for B3LYP energies.<sup>[21]</sup> The optimized geometries for hydrated Tce and Tte forms in solution are given as Electronic Supplementary Information. In the case of Tce, there are only slight changes in the geometry on aqueous solvation. The most noticeable changes are in the O<sub>4</sub>C<sub>3</sub> (+0.016 Å), O<sub>5</sub>C<sub>3</sub> (-0.026 Å), and H<sub>10</sub>O<sub>5</sub> (+0.035 Å) bond lengths, showing that there is some delocalization of charge within the carboxylic group in aqueous solution. Solvation also brings about a degree of nonplanarity in the case of Tte. The changes are larger

here, notably an increase in the hydroxyl H<sub>10</sub>O<sub>5</sub> bond length (+0.045 Å) and concomitant strengthening of the adjacent C<sub>3</sub>O<sub>5</sub> bond (-0.021 Å). Other bond lengths are also affected.

The variation in the bond lengths of the carboxyl group in the isolated, complexed with two water molecules and in bulk water environments for the two conformers, is interesting. Table 2 shows that solvation reduces the C<sub>3</sub>O<sub>5</sub> bond length, but lengthens the other two bonds.

The gas phase vibrational spectrum of Tce is dominated by three regions ( $\sim 1300\text{ cm}^{-1}$ ,  $\sim 1800\text{ cm}^{-1}$ , and  $\sim 3350\text{ cm}^{-1}$ ), corresponding to the stretching frequencies of the —COOH group, along with other vibrations.<sup>[1,4]</sup> Table 2 also shows that the largest modification due to solvation is found in this group. The vibrational frequencies were assigned by analysis of the normal modes. The mode corresponding to the C<sub>3</sub>—O<sub>5</sub> stretch of the COOH group has a lot of mixing from other vibrations. There is resonance of the stretching frequencies of the CO bond of the carboxyl group (C<sub>3</sub>O<sub>5</sub>) and the neighboring carbonyl group (C<sub>2</sub>O<sub>6</sub>), giving rise to two close bands. The values reported in Table 2 correspond to the higher intensity band. The weakening of the O—H (shift =  $-198\text{ cm}^{-1}$ ) and carbonyl ( $-47\text{ cm}^{-1}$ ) bonds for Tce is apparent, but the strengthening of the C<sub>3</sub>O<sub>5</sub> bond is not

**Table 2.** Variation in bond lengths, Wiberg bond orders, stretching frequencies (cm<sup>-1</sup>)<sup>a</sup>, dipole moments (Debye) on solvation for the two conformers Tce and Tte

Bond <sup>b</sup>	Tce	Tce.2H <sub>2</sub> O	Tce.2H <sub>2</sub> O(aq.)	Tte	Tte.2H <sub>2</sub> O	Tte.2H <sub>2</sub> O(aq.)
<b>Length</b>						
C <sub>3</sub> O <sub>4</sub>	1.207	1.216	1.223	1.212	1.218	1.218
C <sub>3</sub> O <sub>5</sub>	1.338	1.322	1.312	1.342	1.322	1.321
O <sub>5</sub> H <sub>10</sub>	0.983	1.006	1.018	0.976	1.017	1.021
<b>Order</b>						
C <sub>3</sub> O <sub>4</sub>	1.759	1.699	1.646	1.750	1.710	1.700
C <sub>3</sub> O <sub>5</sub>	1.085	1.135	1.168	1.077	1.097	1.135
O <sub>5</sub> H <sub>10</sub>	0.684	0.595	0.567	0.718	0.707	0.566
<b>Stretching frequencies</b>						
C <sub>3</sub> O <sub>4</sub>	1802 (188)	1748 (192)	1755 (258)	1760 (313)	1734 (275)	1730 (569)
C <sub>3</sub> O <sub>5</sub>	1375 (126)	1352 (350)	1317 (372)	1112 (231)	1299 (119)	1122 (317)
O <sub>5</sub> H <sub>10</sub>	3420 (99)	3015 (1169)	3222 (301)	3542 (56)	3287 (366)	3024 (406)
<b>Dipole moments</b>						
$\mu$	2.44	6.06	8.07	1.30	2.10	1.07

<sup>a</sup> Values in parenthesis are the respective intensities (km/mol).  
<sup>b</sup> See Fig. 1 for atom numbering.

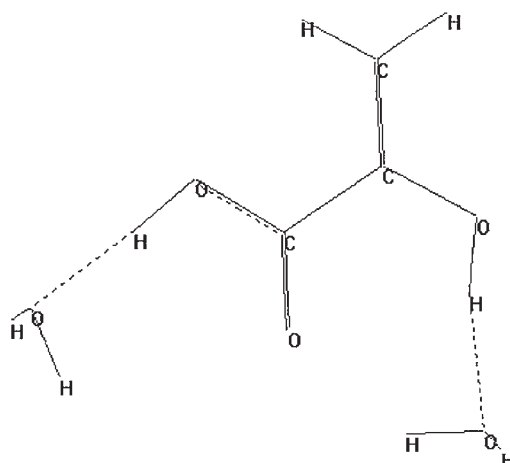


Figure 3. The dihydrate of the enol tautomer

as apparent from the shift in the corresponding band. As mentioned earlier, this band is mixed with other vibrations. A clearer picture emerges from the calculated Wiberg bond orders, also reported in Table 2. A notable increase in the intensity of the O—H band on solvation occurs for both rotamers. This is indicative of the charge redistribution and change in dipole moment in aqueous solution (Table 2).

#### Enol tautomer

The enol tautomer may be a possible intermediate in the decarboxylation to vinyl alcohol. There are various possible forms of this tautomer.<sup>[1]</sup> We performed similar calculations for each of these and found that the structure given in Fig. 3 is the most stable hydrogen-bonded one.

Gas phase calculations at the B3LYP/6-311++G(3df, 3pd)/B3LYP/6-31G(d)<sup>[1]</sup> and PM3 levels suggested that the preferred conformer of the enol tautomer is less stable than *Tce* by 5.9 kcal/mol,<sup>[1]</sup> but in aqueous solution the difference in energies of the two dihydrates reduces to 3.3 kcal/mol. Thus, both the keto and enol tautomers co-exist in solution. The calculated free energy difference in solution of the dihydrates is 6.9 kcal/mol, corresponding to a  $pK_E$  value of 5.03, compared to the experimental value of  $3.21 \pm 0.04$ <sup>[22]</sup> for the keto–enol equilibrium.

#### Other isomers

As for the gas phase,<sup>[1]</sup> we considered two enantiomeric lactone type isomers. On taking the gas phase lactone geometries as initial structures for solvation studies, they optimized to structures that may be termed as protonated pyruvates. Inclusion of explicit water molecules also fails to stabilize the lactone structures, as no intermolecularly hydrogen-bonded structures form with water molecules. In fact, the water molecules move away from the neighborhood of the lactone structures during the MD simulations.

The zwitterionic tautomer, protonated pyruvate,  $\text{CH}_3\text{C}^+(\text{OH})\text{COO}^-$ , has been implicated as a possible intermediate in a proposed mechanism for the interconversion of pyruvate and L-lactate dehydrogenase (EC 1.1.1.27) employing nicotinamide adenine dinucleotide (NAD) as cofactor, according to the

equilibrium:



The reaction involves the transfer of both a proton (to or from an active histidine residue<sup>[23,24]</sup>) and a hydride ion (to or from the cofactor), but whether the reaction is concerted, or, if not, the order of the transfer of the proton and the hydride ion has not yet been established. In the pyruvate-to-lactate direction, if proton transfer to the carbonyl group of pyruvate precedes hydride ion transfer, then 'protonated pyruvate' will be formed as an intermediate. Protonated pyruvate carries a formal positive charge on the central atom, a formal negative charge on the carboxylate group, and is neutrally charged overall. It is actually a tautomer of pyruvic acid in which the acidic proton has been transferred to the carbonyl group. AM1 and *ab initio* SCF/3-21G studies of the conformers of protonated pyruvate and its enantiomeric lactone-type isomers have been reported.<sup>[25]</sup> The isomerization of protonated pyruvate to pyruvic acid is also of general interest in studying the possible mechanisms of decarboxylation of  $\alpha$ -keto acids.<sup>[26]</sup>

Various conformers of protonated pyruvate considered in this work include the ones in which the  $\text{COO}^-$  group is perpendicular to the CCC plane, using initial geometries optimized at the PM3 level.<sup>[1]</sup> On carrying out gas phase calculations, none of the conformers was found to be stable. On geometry optimization, the conformers either optimized to *Tce* or lactone structures, or partially decarboxylated to yield a complex of singlet hydroxyethylidene (methylhydroxycarbene),  $\text{CH}_3\text{COH}$ , and carbon dioxide, separated by a distance of about 3 Å. The same behavior was observed under *ab initio*/STO-3G optimization, although these complexes were found to be stable at the AM1<sup>[25]</sup> and PM3 levels. Optimization of the geometry of the dihydrate structures also yielded the dihydrate of *Tce*. It is gratifying to note that the structure was the same as that obtained earlier (Section 3.1), and this validates our procedure for obtaining initial geometries of the hydrates.

#### Anions

The pyruvate anion is an important intermediate compound in the carbohydrate metabolism of living organisms, and is a product of glycolysis, and a precursor for the Krebs cycle. An adequate understanding of the various interactions in anions can only be obtained by doing calculations using diffuse functions. Accordingly, anion structures were optimized at the B3LYP/6-31+G(d, p) level, followed by single-point calculations at the B3LYP/6-311++G(3df, 3pd) level.

The pyruvate anion may exist as the keto tautomer with the carboxylate group in a planar or nonplanar conformation with respect to the CCC skeleton. Additionally, the methyl hydrogen may be either in a staggered or eclipsed position with respect to the carbonyl group. Calculations for the gas phase suggest that the only conformer of the keto form that has all real vibrational frequencies is shown in Fig. 4.

It is easy to interpret the stability of this conformer, and the existence of imaginary frequencies for the other conformers. The weak attraction between the methyl C—H and the carbonyl group dictates that these two bonds prefer the same plane. However, there is a much stronger repulsion between the carbonyl group and the carboxylate group since all the oxygens are highly negatively charged in the anion. This twists the carboxylate group out of plane, one oxygen going above

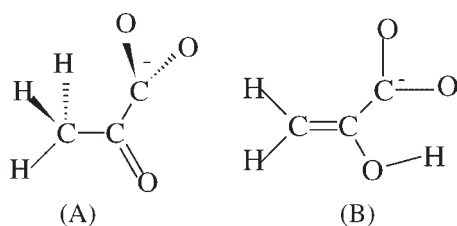


Figure 4. The tautomers of the anion (A): Keto; (B): Enol

the plane and the other going below it. The twist angle between the plane of the carboxylate group and the carbon framework (including the carbonyl group) is  $60.7^\circ$  in the gas phase. The enol tautomer of the anion is found to be less stable than the keto tautomer by only 2.7 kcal/mol in the gas phase (compared to the 5.9 kcal/mol energy difference of the corresponding acids), since it is stabilized by intramolecular hydrogen bonding.

Table 3 gives the charge distribution in *Tce*, anion and the change accompanying anion formation. Large changes are seen at  $C_1$ ,  $C_2$ , and  $O_4$ . It may be noted that there is a large positive charge on the central carbon atom,  $C_2$ , despite the overall negative charge in the anion. The catalytic mechanism of pyruvate decarboxylation involves a nucleophilic attack by the ylide of Thiamin diphosphate (ThDP).<sup>[27]</sup> The large positive charge on the carbonyl carbon atom in solution facilitates the nucleophilic attack.

The calculated gas phase proton affinity for pyruvic acid is 334.5 kcal/mol. This was calculated from the relation  $\Delta H_{\text{ganion}}^0 + \Delta H_{\text{gproton}}^0 - \Delta H_{\text{gTce}}^0$ , where the respective terms are the standard enthalpies of the keto anion, the proton (2.5  $RT$  in the ideal gas approximation), and the undissociated *Tce* form, estimated after making the required thermal corrections to the energy arising from the translational, rotational, and vibrational motions at 298.15 K and 1 atm. This value compares well with the experimentally determined value of  $333.5 \pm 2.9$  kcal/mol.<sup>[22]</sup> The gas phase basicity value, obtained using the corresponding free energy values ( $\Delta G_{\text{ganion}}^0 + \Delta G_{\text{gproton}}^0 - \Delta G_{\text{gTce}}^0$ ), is calculated as 326.1 kcal/mol in comparison with the experimental<sup>[22]</sup> value of  $326.5 \pm 2.8$  kcal/mol. Here,  $S_{\text{gproton}}^0$  was taken as 26.04 kcal/mol.<sup>[28]</sup>

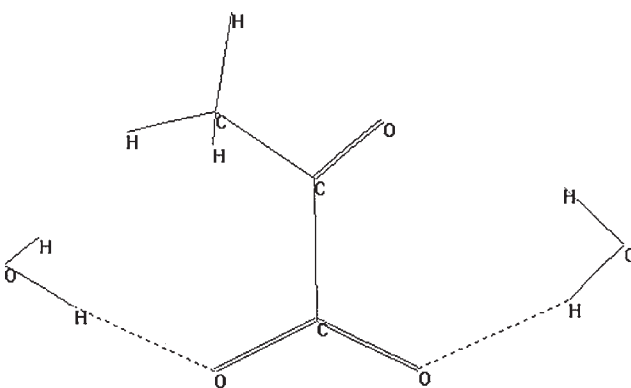


Figure 5. Dihydrate of the anion

The  $\Delta G_{\text{gdeprot,aq}}^0$  value, calculated using the relation,  $\Delta G_{\text{gdeprot,aq}}^0 = \Delta G_{\text{ganion}}^0 + \Delta G_{\text{gproton}}^0 - \Delta G_{\text{gTce}}^0$  is 4.4 kcal/mol, where the aqueous values are obtained by adding the solvation energies to the gas phase values, and the calculated solvation energies of the anion, proton, and pyruvic acid are  $-61.65$ ,  $-264.74$ , and  $-4.70$  kcal/mol, respectively. The corresponding  $pK_a$  value is then 3.26 according to the standard relation,  $pK_a = \frac{1}{2.303RT} \Delta G_{\text{gdeprot,aq}}^0$ . Although the gas phase basicity values are in excellent agreement with the experimental values, the calculated  $pK_a$  value is higher than the experimental value of 2.49 at 298.15 K,<sup>[29]</sup> indicating inadequate treatment of solvation.

Better agreement with the experimental  $pK_a$  value is obtained when the dihydrate is taken for the computation. The structure of the dihydrate of the keto anion is given in Fig. 5. The twist angle in this structure is reduced to  $48^\circ$ . Further solvation in the dielectric medium reduces this angle further to  $37^\circ$ . The calculated  $pK_a$  value is now 3.00, in better agreement with experiment.

The dihydrate of the enol anion is less stable than that of the keto tautomer by 5.5 kcal/mol. Because of the presence of strong intramolecular hydrogen bonding, water is not able to stabilize it to as great an extent as it can stabilize the keto tautomer. Treatment of the dihydrate in aqueous medium increases the energy difference to 7.4 kcal/mol, and it may be concluded that only the keto form of the anion exists in aqueous solution.

Table 3. Calculated change in the partial atomic charges on the various atoms on formation of the anion from *Tce* for pyruvic acid

Atom <sup>a</sup>	Gas			Solution		
	<i>Tce</i>	Anion	$\Delta q$	<i>Tce</i>	Anion	$\Delta q$
$C_1$	-0.137	-0.253	-0.116	-0.161	-0.307	-0.146
$C_2$	0.565	0.441	-0.124	0.614	0.554	-0.060
$C_3$	1.019	1.041	0.022	1.085	1.084	-0.001
$O_4$	-0.692	-0.806	-0.114	-0.757	-0.872	-0.115
$O_5$	-0.697	-0.793	-0.096	-0.753	-0.864	-0.111
$O_6$	-0.708	-0.739	-0.031	-0.748	-0.781	-0.033
$H_7$	0.017	-0.023	-0.040	0.016	0.012	-0.004
$H_8$	0.076	0.058	-0.018	0.083	0.085	0.002
$H_9$	0.076	0.075	-0.001	0.083	0.088	0.005
$H_{10}$	0.481	—	—	0.536	—	—
$\mu$ (D)	2.44	5.26	—	2.75	7.24	—

<sup>a</sup> All calculations at the B3LYP/6-311++G(3df, 3pd)//B3LYP/6-31G(d) level.

## Unimolecular decomposition

Having obtained the stable conformations of pyruvic acid and its tautomers, we investigated its decarboxylation reaction, which has an important biomedical role, since it prevents excessive production of lactic acid resulting from excess of pyruvic acid.

For the gas phase, it was found that the only feasible reaction is decarboxylation to yield acetaldehyde directly, but this reaction has a high energy barrier of 70.1 kcal/mol.<sup>[1]</sup> On calculating the free energy of the transition state in solution, it was found that the free energy of activation in aqueous solution is high (77.3 kcal/mol). This explains the necessity of the catalytic mechanism in reducing the energy barrier for decarboxylation to acetaldehyde.

We also investigated whether decarboxylation to hydroxyethylidene is possible in the aqueous phase, but, as in the gas phase calculations,<sup>[1]</sup> no transition state could be located. Instead, the geometry converged to a twisted *Tce* structure. Finally, the decarboxylation of the enol tautomer to vinyl alcohol was also investigated. In this case, too, no convergence of the transition state could be achieved, and geometry optimization of the transition state led to a twisted protonated pyruvate structure.

## CONCLUSIONS

To summarize the results of this investigation, we may state the following:

Many of the structures, such as the enol tautomer stabilize in aqueous solution and are present to an appreciable extent. The  $pK_E$  value calculated for the equilibrium is in reasonable agreement with the experimental value. The lactone structures, which are found to exist in the gas phase, do not occur in solution. A reason for this is that solvation preferentially stabilizes the lone pairs on the carboxylate oxygens, and hence these oxygens are less available for protonation, which occurs at the carbonyl oxygen instead. As in the gas phase, the favored decarboxylation reaction in solution is the one leading to acetaldehyde, but the barrier to this is even higher than that in the gas phase. The gas phase protonation and basicity values are in good agreement with the experimental values, validating the calculation procedure for the gas phase and the existence of the keto tautomer in both the acid and its anion. The calculated  $pK_a$  value is also in close agreement with the literature value, again validating our calculation methodology for the aqueous phase.

We may thus conclude that the solution phase chemistry of pyruvic acid is completely different from its gas phase chemistry. The energy differences between tautomers are small in aqueous solution, implying that they co-exist.

## Acknowledgements

One of the authors (P.G.) thanks the Council of Scientific and Industrial Research (CSIR), New Delhi, for a research fellowship.

## REFERENCES

- [1] R. Kakkar, M. Pathak, N. P. Radhika, *Org. Biomol. Chem.* **2006**, *4*, 886–895.
- [2] a) E. D. Raczynska, K. Duczmal, M. Darowska, *Pol. J. Chem.* **2005**, *79*, 689–697; b) E. D. Raczynska, K. Duczmal, M. Darowska, *Vibr. Spectrosc.* **2005**, *39*, 37–45.
- [3] X. Yang, G. Orlova, X. J. Zhou, K. T. Leung, *Chem. Phys. Lett.* **2003**, *380*, 34–41.
- [4] I. D. Reva, S. G. Stepanian, L. Adamowicz, R. J. Fausto, *J. Phys. Chem. A* **2001**, *105*, 4773–4780.
- [5] C. Chen, S. F. Shyu, *J. Mol. Struct.: Theochem* **2000**, *503*, 201–211.
- [6] Z. Zhou, D. Du, A. Fu, *Vibr. Spectr.* **2000**, *23*, 181–186.
- [7] Q. Cui, *J. Chem. Phys.* **2002**, *117*, 4720–4728.
- [8] R. Kakkar, A. Dua, S. Zaidi, *Org. Biomol. Chem.* **2007**, *5*, 547–557.
- [9] A. D. Becke, *Phys. Rev. A* **1988**, *38*, 3098–3100.
- [10] C. Lee, W. Yang, R. G. Parr, *Phys. Rev. B* **1988**, *37*, 785–789.
- [11] S. H. Vosko, L. Wilk, M. Nusair, *Can. J. Chem.* **1980**, *58*, 1200.
- [12] M. J. Frisch, G. W. Trucks, H. B. Schlegel, G. E. Scuseria, M. A. Robb, J. R. Cheeseman, J. A. Montgomery, Jr., T. Vreven, K. N. Kudin, J. C. Burant, J. M. Millam, S. S. Iyengar, J. Tomasi, V. Barone, B. Mennucci, M. Cossi, G. Scalmani, N. Rega, G. A. Petersson, H. Nakatsuji, M. Hada, M. Ehara, K. Toyota, R. Fukuda, J. Hasegawa, M. Ishida, T. Nakajima, Y. Honda, O. Kitao, H. Nakai, M. Klene, X. Li, J. E. Knox, H. P. Hratchian, J. B. Cross, C. Adamo, J. Jaramillo, R. Gomperts, R. E. Stratmann, O. Yazyev, A. J. Austin, R. Cammi, C. Pomelli, J. W. Ochterski, P. Y. Ayala, K. Morokuma, G. A. Voth, P. Salvador, J. J. Dannenberg, V. G. Zakrzewski, S. Dapprich, A. D. Daniels, M. C. Strain, O. Farkas, D. K. Malick, A. D. Rabuck, K. Raghavachari, J. B. Foresman, J. V. Ortiz, Q. Cui, A. G. Baboul, S. Clifford, J. Cioslowski, B. B. Stefanov, G. Liu, A. Liashenko, P. Piskorz, I. Komaromi, R. L. Martin, D. J. Fox, T. Keith, M. A. Al-Laham, C. Y. Peng, A. Nanayakkara, M. Challacombe, P. M. W. Gill, B. Johnson, W. Chen, M. W. Wong, C. Gonzalez, J. A. Pople, *Gaussian 03, Revision B.5*, Gaussian, Inc., Pittsburgh PA, **2003**.
- [13] Hypercube, Inc. Florida Science and Technology Park, 1115 N.W. 4th Street, Gainesville, FL, 32601. Web site: <http://www.hyper.com/>
- [14] W. L. Jorgensen, J. Chandrasekhar, J. D. Madura, R. W. Impey, M. L. Klein, *J. Chem. Phys.* **1983**, *79*, 926–935.
- [15] J. J. P. Stewart, *J. Comp. Chem.* **1989**, *10*, 209–220.
- [16] A. P. Scott, L. J. Radom, *J. Phys. Chem.* **1996**, *100*, 16502–16513.
- [17] V. Barone, M. Cossi, *J. Phys. Chem. A* **1998**, *102*, 1995–2001.
- [18] M. Cossi, N. Rega, G. Scalma, V. Barone, *J. Comp. Chem.* **2003**, *24*, 669–681.
- [19] Y. Chiang, A. J. Kresge, P. Pruszynski, *J. Am. Chem. Soc.* **1992**, *114*, 3103–3107.
- [20] E. D. Glendening, A. E. Reed, J. E. Carpenter, F. Weinhold, NBO Version 3.1 (2001) Theoretical Chemistry Institute, University of Wisconsin, Madison.
- [21] L. A. Curtiss, K. Raghavachari, P. C. Redfern, J. A. Pople, *J. Chem. Phys.* **1997**, *106*, 1063–1079.
- [22] S. T. Graul, M. E. Schnute, R. R. Squires, *Int. J. Mass Spectrom. Ion Proc.* **1990**, *96*, 181–198.
- [23] U. M. Grau, W. E. Trommer, M. G. Rossmann, *J. Mol. Biol.* **1981**, *151*, 289–307.
- [24] A. R. Clarke, T. Atkinson, J. J. Holbrook, *Trends Biochem. Sci.* **1989**, *14*, 101–105.
- [25] K. E. Norris, J. E. Gready, *J. Mol. Struct.: Theochem* **1992**, *258*, 109–138.
- [26] R. W. Hanson, *J. Chem. Educ.* **1987**, *64*, 591–595.
- [27] M. A. Lie, L. Celik, K. A. Jørgensen, B. Schiøtt, *Biochemistry* **2005**, *44*, 14792–14806.
- [28] M. W. Chase, Jr., *J. Phys. Chem. Ref. Data* **1998**, Monograph 9: 1–1951.
- [29] A. E. Martell, R. M. Smith, *Critical Stability Constants*, Vol. 3, Plenum Press, NY, **1977**, 66.